Available online at www.sciencedirect.com
SCIENCE DIRECT®
Journal of Nuclear Materials 336 (2005) 22–30
journal of nuclear materials
www.elsevier.com/locate/jnucmat

Structural recovery of self-irradiated natural and ^{238}Pu-doped zircon in an acidic solution at 175 °C

Thorsten Geisler [a,*], Boris Burakov [b], Maria Yagovkina [b], Vladimir Garbuzov [b], Maria Zamoryanskaya [b], Vladimir Zirlin [b], Larisa Nikolaeva [b]

[a] *Institut für Mineralogie, University of Münster, Corrensstrasse 24, 48149 Münster, Germany*
[b] *Laboratory of Applied Mineralogy and Radiogeochemistry, V.G. Khlopin Radium Institute, 28, 2nd Murinskiy ave., St. Petersburg, 194021, Russia*

Received 3 June 2004; accepted 25 August 2004

Abstract

We have investigated the aqueous stability of self-irradiated natural and synthetic ^{238}Pu-doped zircon (4.7 wt% of ^{238}Pu) in an acidic solution at 175 °C. Both zircon samples have suffered a similar degree of self-irradiation damage, as given by their degree of amorphization. X-ray diffraction measurements revealed that during the hydrothermal treatment only the disordered crystalline remnants recovered in the natural zircon, whereas in the ^{238}Pu-doped zircon the amorphous phase strongly recrystallized. Such a different alteration behavior of natural and Pu-doped zircon is discussed in terms of two fundamentally different alteration mechanisms. Our results demonstrate that further experimental studies with Pu-doped zircon are required before any reliable prediction about the long-term aqueous stability of an actinide waste form based on zircon can be made.

1. Introduction

Disposal of highly radioactive materials is a pressing issue in modern society due to the enormous amounts of radioactive waste accumulated world-wide during the past decades from, e.g., dismantled nuclear warheads, atomic icebreakers, and nuclear power plants [1]. In the last 30 years, researchers have considered a number of materials to encapsulate high-level nuclear waste (HLW) for safe permanent disposal such as glasses and crystalline ceramics [2]. Ceramics based on zircon have been suggested for the immobilization of actinides including weapons-grade plutonium [3–5]. However, the radioactive decay of actinides incorporated in zircon causes a transition from a crystalline to a topological disordered (i.e., amorphous) state, which dramatically changes the physical and chemical properties of the material, including its aqueous durablility [4–12].

Hydrothermal experiments with self-irradiation-damaged, natural zircon crystals in acidic, but also neutral solutions produced several micrometer thick alteration zones, even under rather low-temperature conditions [7–12]. It was found that the inward diffusion of hydrogen (as H^+ and/or H_2O) reduces the activation energy of structural recovery processes, which generate a nano-porous structure, as revealed by transmission electron microscopy [12]. These nano-pores enable fast

* Corresponding author. Tel.: +49 251 833 3450; fax: +49 251 833 8397.
E-mail address: tgeisler@nwz.uni-muenster.de (T. Geisler).

0022-3115/$ - see front matter © 2004 Elsevier B.V. All rights reserved.
doi:10.1016/j.jnucmat.2004.08.005

chemical transport through the reaction rim, such that the rate-determining process occurs at the interface. It was suggested that the temperature dependence of the recrystallization of the amorphous phase mainly governs the loss of actinides and other trace elements [9]. Previous experimental work with natural zircon crystals has further demonstrated that radiation-damaged zircon shows a dramatic increase in the alteration rate at two fractions of amorphous domains [11]. Such a critical behavior could be related to the formation of interconnected clusters of amorphous domains and to the percolation of nano-sized regions of depleted matter formed during the α-recoil events, as seen in molecular dynamics simulations and small-angle X-ray scattering experiments [11]. Direct observations of density fluctuations in heavy-ion irradiation tracks in zircon by transmission electron microscopy further support this model [13]. The practical significance of the work was that a fundamental universal property, a percolation threshold, could be proposed as a benchmark of how much radioactive waste can be incorporated into a zircon matrix in order to ensure a safe performance for a particular period.

However, the crucial step in evaluating the suitability of zircon as a waste form is to design representative experiments with synthetic samples doped with ^{238}Pu and ^{239}Pu based on results from less expensive experimental studies on natural analogues. In the present work, we have tried to address this issue by carrying out a hydrothermal experiment in a solution containing 1 M HCl and 1 M $CaCl_2$ at 175 °C with a natural radiation damaged, 5.42×10^8 years old, single zircon crystal from Sri Lanka and a polycrystalline synthetic ^{238}Pu-doped zircon prepared several years before the experiment. During this period, the self-irradiation process in the ^{238}Pu-doped sample has been monitored by X-ray diffraction measurements. Both the natural and the synthetic sample have accumulated a similar degree of self-irradiation damage. The experimental conditions were chosen by taking into account previous published [8,9] and unpublished results of experiments with natural radiation-damaged zircon samples. The main objective of the work presented in this paper was to investigate the behavior of synthetic ^{238}Pu-doped zircon in acidic solutions in comparison with the alteration of natural zircon containing low actinide concentrations.

2. Analytical methods and experimental setup

2.1. Analytical methods

Conventional powder X-ray diffraction (XRD) measurements of the natural zircon were conducted on a Philips X'Pert automated diffractometer using Cu Kα_1 radiation. In order to monitor the recrystallization behavior and to determine the lattice parameters accurately, we added Si as an internal standard. XRD measurements of the ^{238}Pu-doped zircon ceramic were carried out with Co Kα_1 radiation using a special technique developed at the V.G. Khlopin Radium Institute [14]. The highly radioactive ceramic pellet was placed into a regular sample holder, which was hermetically covered by a thin (50–100 μm) partially oxidized Be window. This avoids contamination of the X-ray diffractometer during analysis, but reduces the primary and diffracted intensity and produces additional Be and BeO reflections. The same ceramic pellet was used for all XRD measurements and the hydrothermal experiment.

Immediately after synthesis, one zircon pellet (different to the one used for XRD measurements) was characterized using a Camebax (Cameca) wavelength-dispersive electron microprobe analyzer. The beam current was 10 nA at 20 kV accelerating voltage. A synthetic pure zircon and polycrystalline PuO_2 were used as standards. Matrix corrections were done using the PAP correction procedure.

The experimental solution after the experiment with the ^{238}Pu-doped zircon ceramic was analyzed for ^{238}Pu by gamma spectroscopy using a GWL-90-15 detector. The absolute error of the measurement was 10%.

2.2. Samples

The ^{238}Pu-doped zircon ceramic pellet used in the present work was prepared according to the procedure given in Burakov et al. [15]. XRD analyses indicate that the ceramic pellet contains about 15 wt% tetragonal zirconia. The structural details of the zircon phase after fabrication and at the time of the experiment and the average chemical composition of the zircon phase obtained by multiple electron microprobe measurements are given in Table 1. The zirconia grains in the ceramic were too small (less than 1–2 μm) to allow accurate electron microprobe analyses to be conducted. However, the zirconia phase certainly incorporated some Pu, causing the stabilization of the tetragonal crystalline structure instead of the monoclinic polymorph.

Since the aim of the present study was to compare the effect of radiation damage in natural and synthetic Pu-doped on their aqueous stability, we had to find a natural zircon having suffered a similar degree of damage as the synthetic zircon. It has previously been shown that the amount of amorphous domains controls the degree of alteration under given physico-chemical conditions [11]. The amorphous fraction is thus a good parameter to select a natural zircon for the comparative experiment. The amorphous fraction of the Pu-doped zircon could be estimated from the relative integral intensities of the (2 0 0) zircon peak and the (1 0 1) peak of tetragonal zirconia measured 21 days after fabrication and right before hydrothermal experiments. It was found that the ^{238}Pu-doped zircon was about 60–80% amorphous at

Table 1
Chemical (wt%) and structural parameters, and the age of the ^{238}Pu-doped and natural zircon sample used for the experiments

	Pu-doped zircon (short after fabrication)	Pu-doped zircon (before experiment)	Natural zircon (HZ5) (before experiment)
Zr[a]	46.4 ± 0.4		49.3 ± 0.5
Si[a]	13.5 ± 0.5		14.43 ± 0.04
Hf[a]	–		1.19 ± 0.02
Pu (all isotopes)[a]	5.7 ± 0.2	Not measured	–
^{238}Pu[b]	4.7 ± 0.2		–
P[a]	–		0.02 ± 0.01
Y[a]	–		0.08 ± 0.01
U[c]	–		0.2396 ± 0.0059
Th[c]	–		0.0701 ± 0.0027
Age[c]	21 days	1251 days	542 ± 5 Ma
D ($\times 10^{18}$ α/g)[d]	0.07	3.9	4.7 ± 0.1
D ($\times 10^{24}$ α/m^3)	0.3	18.8	20.2 ± 0.7
f_a (%)[e]	<5	60–80	70 ± 7
a_0 (nm)	0.6639 ± 0.0010	0.6708 ± 0.0021[f]	0.6676 ± 0.0014
c_0 (nm)	0.6014 ± 0.0020	0.6143 ± 0.0053	0.6063 ± 0.0047
δ (g/cm^3)[g]	4.76	–	4.30 ± 0.06

Errors are given at the two-sigma level.

[a] The chemical composition was determined by multiple electron microprobe measurements. The data of the natural zircon are from Geisler et al. [10].

[b] Calculated from the isotopic composition of the Pu.

[c] U and Th concentration and the ^{207}Pb/^{206}Pb age of the natural zircon were determined by sensitive high-resolution ion microprobe [10].

[d] For the ^{238}Pu-doped zircon, the dose was estimated from the calculated density.

[e] The amorphous fraction of the Pu-doped zircon was estimated from the intensity ratio of the (200) peak of zircon and the (101) peak of t-(Zr,Pu)O_2 by assuming that the intensity of the zirconia peaks did not change after fabrication (see Fig. 3). The amorphous fraction of the natural zircon is from Geisler et al. [11].

[f] Since the Bragg intensity is dramatically reduced in highly damaged samples (Fig. 3), the unit-cell constants of the Pu-doped zircon prior to the experiment were estimated by first calculating the a constant from the position of the strong (200) reflection and the quadratic equation for $hk0$. The c constant was then estimated by using the value for a and the position of the (112) reflection. The errors of both parameters are thus highly correlated.

[g] The density of the Pu-doped zircon was calculated from the unit-cell volume obtained from the X-ray diffraction measurements and the chemical composition. The density of sample HZ5, however, was measured by conventional immersion technique using water as immersion fluid.

the time of the hydrothermal experiment (Table 1). The amorphous fraction of a suite of natural, gem-type zircon from Sri Lanka has been directly measured by XRD, infrared, and nuclear magnetic resonance techniques and calibrated against the α-decay dose [16–18]. It was thus possible to select a natural zircon from Sri Lanka for the experiment based on this calibration and the measured α-decay dose. The selected natural zircon (HZ5) has accumulated a dose of $(4.7 \pm 0.1) \times 10^{18}$ α-decays/g and is about 70% amorphous [10,11]. Chemical and structural details of this zircon sample are summarized in Table 1.

2.3. Experimental setup

The hydrothermal experiments were carried out in Teflon reactor vessels with a solution containing 1 M HCl and 1 M $CaCl_2$. Such solution has been used in previous studies with natural zircon, which have shown that significant reactions can be expected within laboratory time scales [8]. A special steel autoclave with an internal Teflon reactor vessel (Fig. 1) was used at V.G. Khlopin

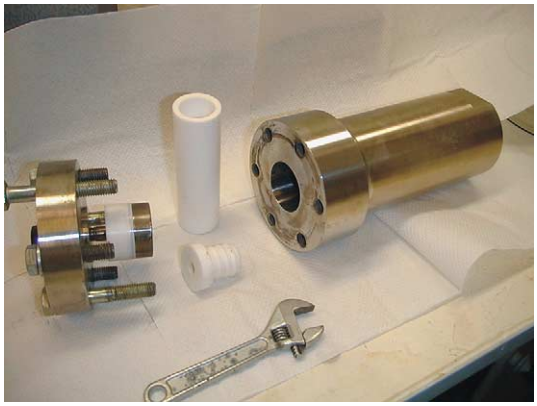

Fig. 1. Steel autoclave with a Teflon reactor vessel (white cylinder) used for experiments with ^{238}Pu-doped ceramic sample at the V.G. Khlopin Radium Institute.

Radium Institute for the experiment with the ^{238}Pu-doped zircon. The ceramic specimen was placed on a 'pillow' of platinum to avoid contact of the pellet with the Teflon. We used 5 and 35 ml of solution for the experiment with the natural and the Pu-doped zircon, respectively. The experiment with the natural zircon was conducted with 0.1 g powder of grain sizes <50 μm and a larger grain with a polished surface, which has been used to study the reaction rim by backscattered electron (BSE) imaging. The vessels were placed in an oven and heated to (175 ± 3) °C for 14 days.

3. Results and discussion

3.1. Self-irradiation damage effects in ^{238}Pu-doped zircon

The increasing degree of self-irradiation damage in the zircon phase after its fabrication causes the intensity of the diffraction peaks to decrease, their width to increase, and their position to shift to low two-theta angles (Fig. 2). Such a behavior is known from numerous studies on natural and synthetic zircon [4–6,19,20]. In contrast, the shape, position, and intensity of the diffraction peaks from the tetragonal $(Zr,Pu)O_2$ phase did not change significantly (Fig. 2), confirming that zirconia is extremely resistant to self-irradiation, i.e., it cannot be amorphized [21]. This observation has recently been explained by the inability to form an alternative covalent ZrO_2 network [22].

Fig. 3 shows a Williamson–Hall plot [23] for the zircon phase at different degree of damage. The Williamson–Hall plot is used to assess the broadening of the diffraction peak arising from small grain size and/or internal strain. In this plot, the full width at half maximum (b) is shown as a function of the diffraction angle θ, i.e., $b\cos\theta$ is plotted as a function of $\sin\theta$, and is represented by

$$b\cos\theta = \lambda/L + \varepsilon\sin\theta. \quad (1)$$

A linear extrapolation of the data to the intercept of the ordinate axis gives λL, with λ being the wavelength of the radiation used and L the diameter of the grains in a polycrystalline sample. The slope of the best-fit line gives an estimation of the internal strain ε. Due to the low intensity arising from X-ray absorption in the Be window and overlap with BeO and Be peaks, only four to six peaks could be used. However, it is evident from Fig. 3 that crystallite size effects became important after a dose of $1.36 - 1.91 \times 10^{18}$ α-decays/g. This observation is consistent with a single-crystal X-ray diffraction study of natural zircons, which has shown that after the first percolation point has been reached, i.e., after amorphous domains start to form an interconnected network, strain broadening becomes less important with respect to crystallite size broadening effects [24].

As shown in Fig. 4(a), a near-linear relationship exists between the lattice parameters of the ^{238}Pu-doped zircon. Furthermore, in contrast to the anisotropic expansion of the lattice constants seen in natural zircon from Sri Lanka, which has been attributed to point

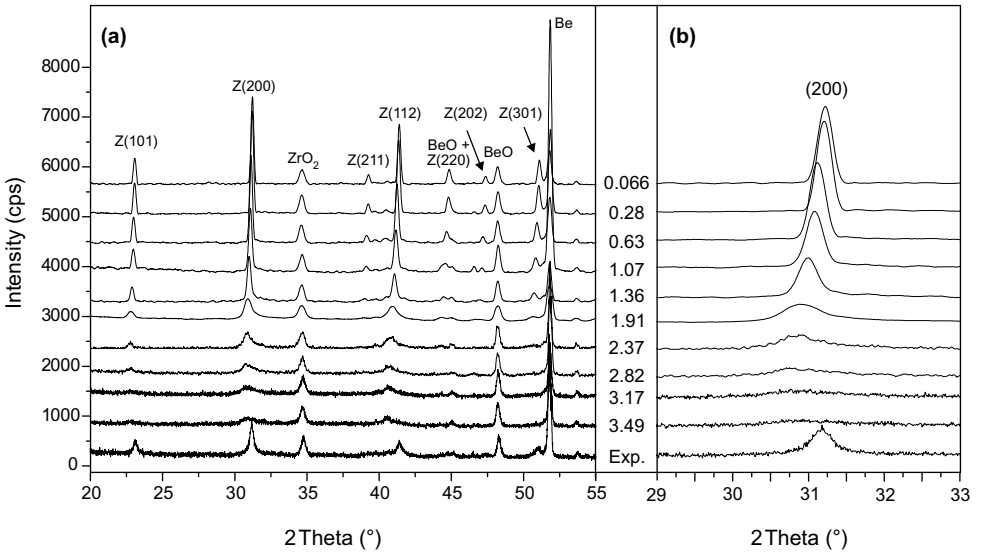

Fig. 2. Stacked X-ray diffraction patterns (Co Kα radiation) of the ^{238}Pu-doped zircon ceramic measured after the accumulation of different self-irradiation doses (given in 10^{18} α-decays/g) and after the hydrothermal treatment (labeled 'Exp.'): (a) between 20° and 55° 2θ and (b) between 29° and 30° 2θ, showing the (200) peak of zircon. Diffraction peaks from zircon (Z), tetragonal zirconia (ZrO_2), and from the Be window (Be and BeO) are indicated.

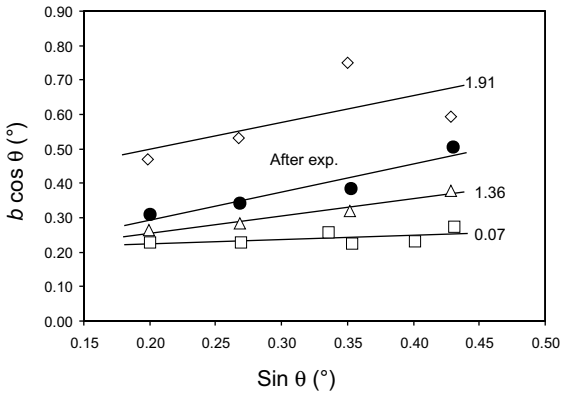

Fig. 3. Williamson–Hall plot for the ^{238}Pu-doped zircon after the accumulation of three different self-irradiation doses (given in 10^{18} α-decays/g) and after the hydrothermal treatment. The full width at half maximum (b) was not corrected for instrumental broadening. Note the strong increase of the crystallite size effect on the peak broadening at a dose of 1.91×10^{18} α-decays/g.

defect annealing over geological time scales [19,20], the unit-cell parameters of ^{238}Pu-doped zircon increase isotropically with increasing α-decay dose (Fig. 4(a)). Our results are in full agreement with data of Weber [20] from ^{238}Pu-doped zircon. It is worth pointing out that the unit-cell volume swelling of Pu-doped and natural zircon from Sri Lanka proceeded approximately with a similar rate when considering available XRD data of natural zircon (Fig. 4(b)). This is surprising because unambiguous Raman spectroscopic evidences have been reported by Nasdala et al. [25], showing that some annealing occurred during the geological history of the Sri Lanka zircon crystals. Based on the comparison of the linewidth of the asymmetrical $v_3(SiO_4)$ stretching band as a function of dose between annealed and unannealed zircon, these authors suggested that the α-decay dose should be corrected by a factor of 0.55 to estimate an 'effective dose'. It is evident from Fig. 4(b) that this correction would result in a significantly larger unit-cell volume-swelling rate for natural than for synthetic ^{238}Pu-doped zircon. The reason for this apparent discrepancy is not yet clear. However, based on these results it follows that the use of a corrected ('effective') dose as suggested by Nasdala et al. [25] to compare self-irradiation damage effects in natural and synthetic Pu-doped zircon is not justified.

3.2. Hydrothermal annealing of radiation-damaged natural and ^{238}Pu-doped zircon

Fig. 5 shows optical micrographs of the Pu-doped zircon pellet before and after hydrothermal treatment. These images did not reveal any differences between the treated and the untreated zircon pellet, indicating

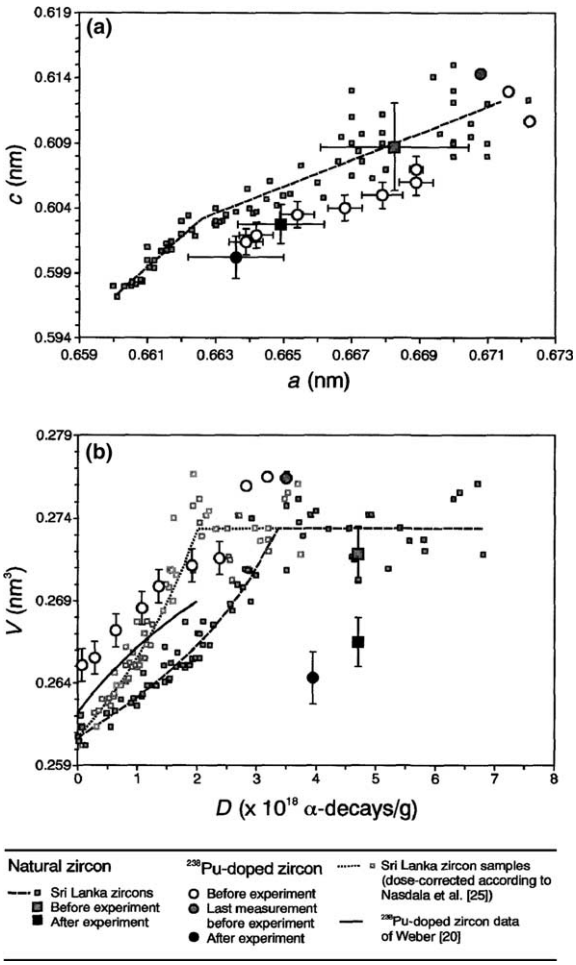

Fig. 4. (a) The c-axis as a function of the a-axis and (b) the unit-cell volume as a function of the α-decay dose for untreated and hydrothermally treated natural and ^{238}Pu-doped zircon. The dotted and stippled line are guides to the eyes only to better visualize the trend directions of the dose corrected (i.e., the α-decay dose was multiplied by 0.55 according to Nasdala et al. [25]) and the uncorrected data of the natural zircon samples (data from [6,7,22,24,38–40]), respectively. Error bars represent the one-sigma standard deviation.

that significant disintegration and congruent dissolution did not take place during the experiment. After a cumulative dose 3.9×10^{18} α-decays/g (right before the hydrothermal experiment) none of the ceramic pellets has shown any evidence for newly formed cracks. One thin crack, which can be seen at the surface of ceramic pellet used for XRD analyses and the hydrothermal experiment (Fig. 5(c) and (d)), was initially formed during sintering. The hydrothermal treatment neither affected this initial crack nor caused the formation of new cracks.

However, the reoccurrence of strong zircon diffraction peaks in the X-ray diffraction pattern (Fig. 2) shows

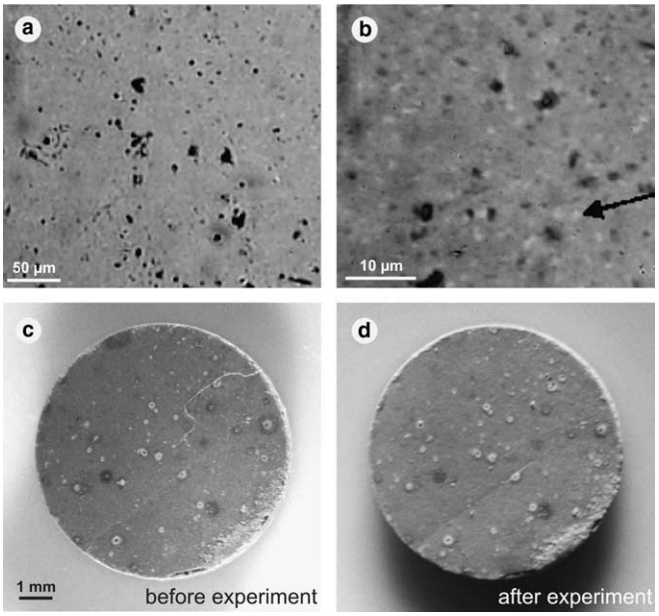

Fig. 5. (a) and (b) reflected light micrographs of the pellet after fabrication, (c) optical micrograph of the whole pellet prior to the hydrothermal experiment and (d) after the experiment. Arrow in (b) points to a tetragonal zirconia grain.

that significant structural recovery occurred during the experiment. Unit-cell refinement revealed a significant decrease of the lattice constants of zircon, which are close to or even smaller than those obtained immediately after ceramic fabrication (Fig. 2). However, the recovered zircon lattice is still significantly more strained than the undamaged zircon ceramic, as shown by the Williamson–Hall plot in Fig. 3. We further emphasize that we could not detect any new phase in the XRD pattern.

The most surprising result of the present study is, however, that the treatment of the self-irradiated ^{238}Pu-doped zircon has activated significant recrystallization at the expense of the amorphous phase, whereas no recrystallization occurred in the natural zircon. This is illustrated in Fig. 6 by exemplarily analyzing the shape and intensities of the (200) zircon peak of the hydrothermally treated samples. In Fig. 6(a), we have scaled the intensities of the (200) peak from the treated and untreated Pu-doped zircon pellet by using the (101) peak of tetragonal zirconia, $(Zr,Pu)O_2$. We note that the stacked diffraction patterns shown in Fig. 2 demonstrate that the intensity of this peak did not change significantly, neither during the damage process nor during the hydrothermal treatment. This suggests that the zirconia can be considered as an internal standard. This observation also shows that tetragonal zirconia is very stable under the conditions of the experiment. Aside from the clear shift of the maximum of the (200) zircon peak to higher 2θ-values, it is evident from Fig. 6(a) that its intensity increased significantly, clearly indicating that recrystallization occurred. From the integral intensity ratio between the (200) zircon and the (101) zirconia peak, we can roughly estimate that only about 30% amorphous remnants must have survived within the analyzed volume. We recall that under dry conditions temperatures in excess of 700 °C are needed to recrystallize the amorphous phase in natural and Pu-doped zircon [26–28].

In the case of the natural zircon, the situation is completely different (Fig. 6(b)). The untreated natural zircon shows a broad asymmetric peak with the slower decay occurring at the higher two-theta side. Such peaks were deconvoluted by two pseudo-Voigt functions, and the unit-cell parameters were obtained from the most intense contribution of the profile. The peak asymmetry has previously been attributed to result from the amorphous phase [6]. However, in a recent study of partially damaged crystals, it could be shown that the asymmetry is clearly related to the occurrence of compressed crystalline regions, which are possibly located within the boundary between expanded crystalline and amorphous regions [29]. The amorphous phase itself could not be detected in both the natural and the ^{238}Pu-doped zircon with our equipment because of the low intensity of the signal.

After the hydrothermal treatment, the integral intensity of the (200) peak, normalized to the (111) peak of silicon (mixed in equal amounts to the samples), has not changed (Fig. 6(b)), demonstrating that the amorphous

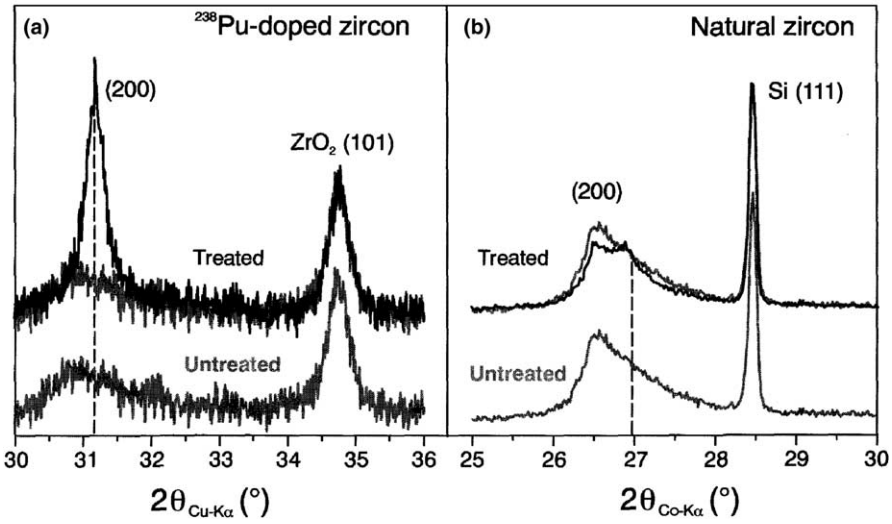

Fig. 6. Peak profile for the (200) reflection of (a) the untreated and the hydrothermally treated ^{238}Pu-doped zircon (Co Kα radiation) and (b) the natural zircon from Sri Lanka (Cu Kα radiation). To allow for a better comparison, the profiles of the untreated sample are additionally put under the profiles of the treated sample using a grey line. Vertical grey stippled lines mark the position of crystalline $ZrSiO_4$ and (Zr,Pu)SiO_4, respectively. Note that compressed crystalline regions can clearly be detected in the natural zircon, resulting in a peak asymmetry.

material did not recrystallize during the experiment. The treatment merely caused the partial recovery of the expanded crystalline domains, as shown by a new peak at higher two-theta values in the profile of the treated material. In addition, some compressed regions were relaxed as can be seen by slight changes in the shape of the asymmetry of the peak profile. However, the unit-cell constants, refined from the peak maximum of this contribution obtained by fitting a third pseudo-Voigt function to the profile, are still larger than those of an undamaged synthetic zircon (Figs. 3 and 4).

BSE images of the reacted natural zircon reveal that the X-ray diffraction profile of the treated sample can be understood as representing a mixture of contributions from a reaction rim and an unreacted core (Fig. 7). The reaction rims penetrate 5–10 μm into the grains and show a scalloped front morphology. They are characterized by a lower BSE intensity, which was shown to be the result of an exchange of Si and Zr with Ca and hydrogen [8–10,12]. Our new data of experimentally altered, natural zircon are fully consistent with the previously proposed diffusion-reaction (recrystallization) model, which is based on the diffusion of hydrogen (H^+ and/or H_2O) into the amorphous network [7–12].

The degree of alteration of the ^{238}Pu-doped zircon was estimated from the amount of ^{238}Pu released into solution after hydrothermal treatment as measured by gamma spectroscopy. The ^{238}Pu content was 8.8×10^{-6} g/ml, corresponding to a total ^{238}Pu loss of 3.1×10^{-4} g. Normalized Pu mass loss calculated without correction for ceramic porosity was 2.5 g/m^2 of sample surface. From the Pu mass loss and geometric surface area of the pellet, we have estimated a minimum apparent reaction rim thickness (x_{min}) in the treated ^{238}Pu-doped zircon ceramic from

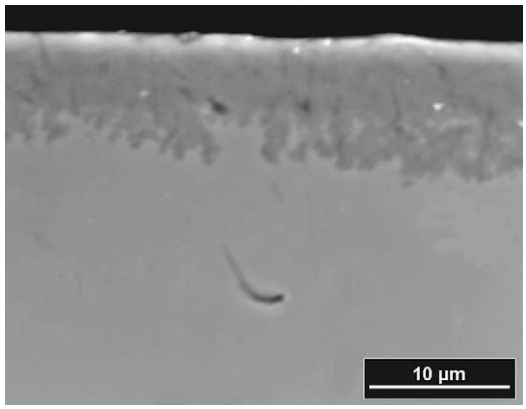

Fig. 7. Backscattered electron image of the hydrothermally treated grain from the natural zircon sample (HZ5). The reaction rim is characterized by a lower BSE intensity and a scalloped front morphology.

$$V_a = V_p - \pi(r - x_{min})^2(h - x_{min}), \quad (2)$$

where V_p and V_a is the volume of the ceramic pellet and the volume affected by the alteration, respectively, r is the radius of the pellet ($r = 0.383$ cm), and h is its height ($h = 0.13$ cm). Here we also assume (1) an 8% macroscopic volume swelling of the zircon phase prior to the experiment [20], and (2) that all ^{238}Pu within the reacted

volume has been lost to the fluid (i.e., $V_a \approx 0.00151\,cm^3$). The calculation yields a minimum apparent rim thickness of about 20 μm, which is about twice the measured rim thickness of the treated natural zircon (Fig. 7). Assuming that the effect of the ceramic porosity is partly counterbalanced by the occurrence of zirconia, this value seems to be a reasonable estimate for $x_{min.}$

At the first glance, one may attribute the observed difference in the degree of alteration and recrystallization in both samples to differences in the kinetics of the process. However, it is not obvious why the kinetics of recrystallization of amorphous zircon (i.e., epitaxial growth of crystalline remnants) should be significantly different in natural and synthetic ^{238}Pu-doped zircon having a similar degree of self-irradiation damage. A key to the explanation of this observation is given by a recent review of replacement reactions of Putnis [30]. This author has shown that many replacement reactions take place principally by a coupled dissolution–reprecipitation process, where dissolution is believed to be coupled with precipitation of a thermodynamically more stable phase or a phase assemblage. This often results in pseudomorphism, where the crystallographic shape of the parent is preserved. Recent experimental work has revealed that the contact of a solid solution with a fluid, which is supersaturated with respect to elements of the other compositional end member can potentially cause the replacement of this phase by a new phase of mixed composition, which is momentarily in local equilibrium with the fluid [31,32]. While a sharp replacement front moves into the parent, the new phase evolves in structure and composition towards the end member as long as the reaction proceeds. Evidence for such a process was also found in natural zircon enriched in rare earth elements, which became unstable during the interaction with a metamorphic fluid and was replaced by REE-depleted zircon [33]. It is thus conceivable that the Pu-rich amorphous phase as well as the disordered crystalline remnants dissolved while new zircon with less Pu precipitated simultaneously. Consequently, the solubility of (Zr,Pu)SiO_4 (amorphous and crystalline) and of the $PuSiO_4$ end member must have been higher than that of Pu-poor $ZrSiO_4$. This can be explained by the fact that, although $PuSiO_4$ is isostructural with $ZrSiO_4$, a large miscibility gap even at high temperatures is expected to exist [15,34], resulting in a high excess enthalpy of mixing at low temperatures. It is well known for solid solution–aqueous solution systems that an excess enthalpy (i.e., an excess Gibbs energy) of mixing of a regular solid solution can increase the solubility of a solid solution at thermodynamic equilibrium relative to an ideal solid solution, but also relative to a solid solution with a lower mole fraction of one component if the solubility of both end members is of the same order of magnitude [35].

The described coupled dissolution–reprecipitation process is fundamentally different to the diffusion-reaction model used to describe experimental aqueous alteration of natural radiation-damaged zircon [7–12], but can explain the observed significant difference in the recrystallization rate and the fact that no change of the surface morphology of the pellet has been observed. A Pu-poor zircon is expected to have smaller lattice constants ($a = 0.6607$ nm and $c = 0.5982$ nm for $ZrSiO_4$ [36] and $a = 0.6906$ nm and $c = 0.6221$ nm for the $PuSiO_4$ end member [37]). Unfortunately, our X-ray diffraction measurements are neither precise enough to confirm nor to reject such expectation (see Fig. 4). The higher apparent rim thickness in the Pu-doped zircon further points to dissolution–reprecipitation mechanism, which is believed to be controlled by a much faster moving interface than diffusion processes. However, since we have estimated the reaction rim thickness from the concentration of ^{238}Pu in solution only, we cannot rule out that the existence of grain boundaries allowed deeper penetration of the fluid into the ceramic pellet.

4. Concluding remarks

The most important result of our study is that the behavior of self-irradiated natural and ^{238}Pu-doped synthetic zircon in an acidic solution was found to be significantly different. Whereas alteration of natural radiation-damaged zircon with a low doping level of U and Th is controlled by diffusion-reaction processes, the high recrystallization rate observed in synthetic radiation-damaged zircon doped with a high amount of Pu is compatible with the concept of a coupled dissolution–reprecipitation process, where dissolution occurs simultaneously with reprecipitation at a moving front. Whatever the mechanism, our findings have strong implications for the assessment of the suitability of zircon as a nuclear waste form as they show that studies on 'real case' synthetic samples are indispensable before any confidential predictions about the long-term aqueous stability of an actinide waste form with zircon host matrix can be made. We conclude that the influence of high actinide doping levels on the aqueous stability has to be considered when evaluating the suitability of zircon as a waste form based on experimental data or mineralogical observations on natural zircon containing low amounts of impurities.

Acknowledgments

Experiments with ^{238}Pu-doped sample were supported in part by the V.G. Khlopin Radium Institute. We are grateful to A. Alexeev of the V.G. Khlopin Radium Institute for the analysis of Pu contents in ceramic and solution by gamma spectrometry and to A. Breit of the Mineralogical Institute of the University of Münster

for carrying out the X-ray diffraction measurements on the natural zircon. K. Pollok and F. Tomaschek are thanked for many fruitful discussions. We would also like to thank A. Janssen of the Mineralogical Institute of the University of Münster for his help with the hydrothermal experiment on the natural zircon, the Mineralogical Museum of the University of Hamburg for providing the natural zircon sample and the Deutsche Forschungsgemeinschaft (GE 1094/4-1) for financial support.

References

[1] W. Stoll, Mater. Res. Bull. 23 (1998) 6.
[2] W. Lutze, R.C. Ewing, Radioactive Waste Forms for the Future, Amsterdam, North-Holland, 1988.
[3] B.E. Burakov, Process Saf. waste 93 (2) (1993) 19.
[4] R.C. Ewing, W. Lutze, W.J. Weber, J. Mater. Res. 10 (1995) 243.
[5] R.C. Ewing, Proc. Natl. Acad. Sci. USA 96 (1999) 3432.
[6] T. Murakami, B.C. Chakoumakos, R.C. Ewing, G.R. Lumpkin, W.J. Weber, Am. Mineral. 76 (1991) 1510.
[7] T. Geisler, M. Ulonska, H. Schleicher, R.T. Pidgeon, W. van Bronswijk, Contrib. Mineral. Petrol. 141 (2001) 53.
[8] T. Geisler, R.T. Pidgeon, W. van Bronswijk, R. Kurtz, Chem. Geol. 191 (2002) 141.
[9] T. Geisler, M. Zhang, E.K.H. Salje, J. Nucl. Mater. 320 (2003) 280.
[10] T. Geisler, R.T. Pidgeon, R. Kurtz, W. van Bronswijk, H. Schleicher, Am. Mineral. 86 (2003) 1496.
[11] T. Geisler, K. Trachenko, S. Ríos, M. Dove, E.K.H. Salje, J. Phys: Condens. Matter 15 (2003) L597.
[12] T. Geisler, A.-M. Seydoux-Guillaume, M. Wiedenbeck, R. Wirth, J. Berndt, M. Zhang, B. Mihailova, A. Putnis, E.K.H. Salje, J. Schlüter, Am. Mineral. 89 (2004) 1341.
[13] L.A. Bursill, G. Braunshausen, Philos. Mag. A 62 (1990) 395.
[14] B.E. Burakov, E.B. Anderson, Excess Weapons Plutonium Immobilization in Russia, in: J.L. Jardine, G.B. Borisov (Eds.) Proceeding Meeting for Coordination and Review of Work, St. Petersburg, Russia, UCRL-ID-138361, 2000 p. 167.
[15] B.E. Burakov, E.B. Anderson, M.V. Zamoryanskaya, M.A. Yagovkina, E.E. Strykanova, E.V. Nikolaeva, M.R.S. Symp. Proc. 663 (2001) 307.
[16] S. Ríos, E.K.H. Salje, M. Zhang, R.C. Ewing, J. Phys.: Condens. Matter 12 (2000) 2401.
[17] I. Farnan, E.K.H. Salje, J. Appl. Phys. 89 (2001) 2084.
[18] M. Zhang, E.K.H. Salje, J. Phys.: Condens. Matter 13 (2001) 3057.
[19] H.D. Holland, D. Gottfried, Acta Cryst. 8 (1955) 291.
[20] W.J. Weber, Radiat. Eff. 115 (1991) 341.
[21] K.E. Sickafus, Hj. Matzke, Th. Hartmann, K. Yasuda, J.A. Valdez, P. Chodak III, M. Nastasi, R.A. Verrall, J. Nucl. Mater. 274 (1999) 66.
[22] K. Trachenko, M.T. Dove, M. Pruneda, E. Artacho, E.K.H. Salje, T. Geisler, I. Todorov, B. Smith, M.R.S. Symp. Proc. 792 (2004), R6.2.1.
[23] G.K. Williamson, W.H. Hall, Acta Metall. 1 (1953) 22.
[24] E.K.H. Salje, J. Chrosch, R.C. Ewing, Am. Mineral. 84 (1999) 1107.
[25] L. Nasdala, P.W. Reiners, J.I. Garver, A.K. Kennedy, R.A. Stern, E. Balan, R. Wirth, Am. Mineral. 89 (2004) 219.
[26] M. Zhang, E.K.H. Salje, I. Farnan, G.C. Capitani, H. Leroux, A.M. Clark, J. Schlüter, J. Phys. Condens. Matter 12 (2000) 3131.
[27] T. Geisler, Phys. Chem. Miner. 29 (2002) 420.
[28] B.D. Begg, N.J. Hess, W.J. Weber, S.D. Conradson, M.J. Schweiger, R.C. Ewing, J. Nucl. Mater. 278 (2000) 212.
[29] S. Ríos, T. Boffa-Ballaran, J. Appl. Cryst. 36 (2003) 1006.
[30] A. Putnis, Mineral. Mag. 66 (2002) 689.
[31] A.E. Glikin, S.I. Kovalev, E.B. Rudneva, L.Yu. Kryuchkova, A.E. Voloshin, J. Cryst. Growth 255 (2003) 150.
[32] C. Putnis, K. Mezger, Geochim. Cosmochim. Acta 68 (2004) 2839.
[33] F. Tomaschek, A.K. Kennedy, I.M. Villa, M. Lagos, C. Ballhaus, J. Petrol. 44 (2003) 1977.
[34] S.V. Ushakov, W. Gong, M.M. Yagovkina, K.B. Helean, W. Lutze, R.C. Ewing, Ceram. Trans. 93 (1999) 357.
[35] P. Glynn, Rev. Miner. Geochem. 40 (2000) 481.
[36] K. Robinson, G.V. Gibbs, P.H. Ribbe, Am. Mineral. 56 (1971) 782.
[37] C. Keller, Nukleonik 5 (1963) 4.
[38] J.A. Woodhead, G.R. Rossman, L.T. Silver, Am. Mineral. 76 (1991) 74.
[39] M. Zhang, E.K.H. Salje, R.C. Ewing, I. Farnan, S. Ríos, J. Schlüter, P Leggo, J. Phys.: Condens. Matter 12 (2000) 5189.
[40] R. Biagini, I. Memmi, F. Olmi, N. Jahrb, Miner. Monatsh. 1997 (1997) 257.